MASTER COPY

OAK RIDGE NATIONAL LABORATORY
operated by
UNION CARBIDE CORPORATION
for the
U.S. ATOMIC ENERGY COMMISSION

ORNL-TM-230

COPY NO. - 84

DATE - May 10, 1962

SUPER-PROMPT-CRITICAL BEHAVIOR OF AN UNMODERATED, UNREFLECTED URANIUM-MOLYBDENUM ALLOY ASSEMBLY

J. T. Mihalczo

Abstract

The time-dependent behavior of the neutron population in an unreflected, unmoderated cylindrical assembly of a 90 wt% uranium (93.2 wt% U^{235}), 10 wt% molybdenum alloy following a rapid establishment of a super-prompt critical condition with negligible initial neutron population has been investigated to support the design of a reactor capable of producing bursts of 10^{17} fissions. Reactivity increases up to 11 cents above prompt critical resulted in bursts yielding as many as 1.8×10^{17} fissions with reactor periods as short as 16 μsec and temperature increases as large as 400°C. Pressure waves generated in a portion of the core held in position by an electromagnet for bursts greater than $\sim 6 \times 10^{16}$ fissions initiated the removal of this section of the core about 225 μsec after the peak of the burst.

NOTICE

This document contains information of a preliminary nature and was prepared primarily for internal use at the Oak Ridge National Laboratory. It is subject to revision or correction and therefore does not represent a final report. The information is not to be abstracted, reprinted or otherwise given public dissemination without the approval of the ORNL patent branch, Legal and Information Control Department.

LEGAL NOTICE

This report was prepared as an account of Government sponsored work. Neither the United States, nor the Commission, nor any person acting on behalf of the Commission:

A. Makes any warranty or representation, expressed or implied, with respect to the accuracy, completeness, or usefulness of the information contained in this report, or that the use of any information, apparatus, method, or process disclosed in this report may not infringe privately owned rights; or

B. Assumes any liabilities with respect to the use of, or for damages resulting from the use of any information, apparatus, method, or process disclosed in this report.

As used in the above, "person acting on behalf of the Commission" includes any employee or contractor of the Commission, or employee of such contractor, to the extent that such employee or contractor of the Commission, or employee of such contractor prepares, disseminates, or provides access to, any information pursuant to his employment or contract with the Commission, or his employment with such contractor.

Introduction

The design of a bare metal reactor intended to produce high-intensity bursts of neutrons having a near-fission spectrum has been described by Breidenbach et al.[1] Similar in principle to the Los Alamos Lady Godiva and Godiva II bare U^{235} reactors, the present design obtains greater strength and improved physical characteristics through the use of a 90 wt% uranium - 10 wt% molybdenum alloy in its construction. The uranium is enriched to 93.2 wt% U^{235}.

A previous paper[2] described a series of zero-power experiments with this assembly. Those results included reactivity calibrations of various parts, fission-rate distributions, and reactivity effects of reflective materials near the reactor.

The time behavior of the reactor during super-prompt-critical neutron bursts of various sizes is described here. All experiments were conducted indoors at the ORNL Critical Experiments Facility. Reactor periods, burst shapes, temperature changes, leakage fluxes, and fission yields were measured. The observed bursts were compared to theoretical predictions derived from the one-group, space-independent model given by Wimett et al.[3]

Description of Apparatus

The assembly used in these experiments is the ORNL Health Physics Research Reactor (HPRR). It is essentially a 20.32-cm-dia by 23-cm-high cylinder of uranium-molybdenum alloy with a 5-cm-dia steel core. A detailed drawing of the reactor is shown as Fig. 1, and Figs. 2 and 3 are photographs of the final assembly.

An 8.6-cm-OD annulus, containing 9.4 kg of the total 96.6 kg of U^{235} in the reactor, is attached to the lower end of the magnetically supported steel core and serves as a safety block. A motor drive moves the magnet

---

1. G. Breidenbach et al., Preliminary Design of the ORNL Fast Burst Reactor, NDA-2136-1 (July 30, 1960).
2. J. T. Mihalczo, Reactivity Calibrations and Fission-Rate Distributions of an Unmoderated, Unreflected Uranium-Molybdenum Alloy Research Reactor, ORNL-TM-189 (to be published).
3. T. F. Wimett et al., Nuclear Sci. and Eng. 8, 691 (1960).

UNCLASSIFIED
ORNL-LR-DWG 65369

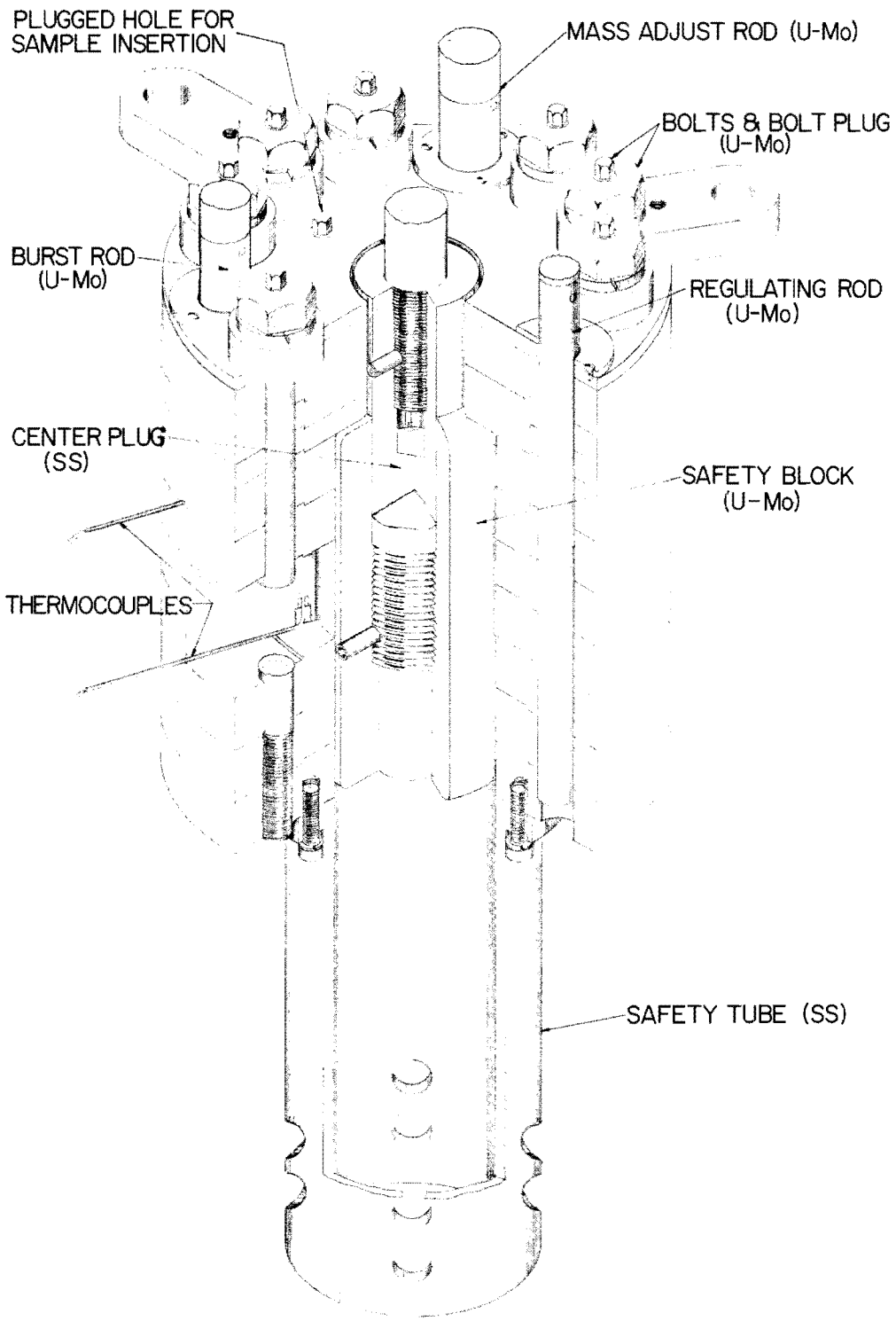

Fig. 1. ORNL Health Physics Research Reactor.

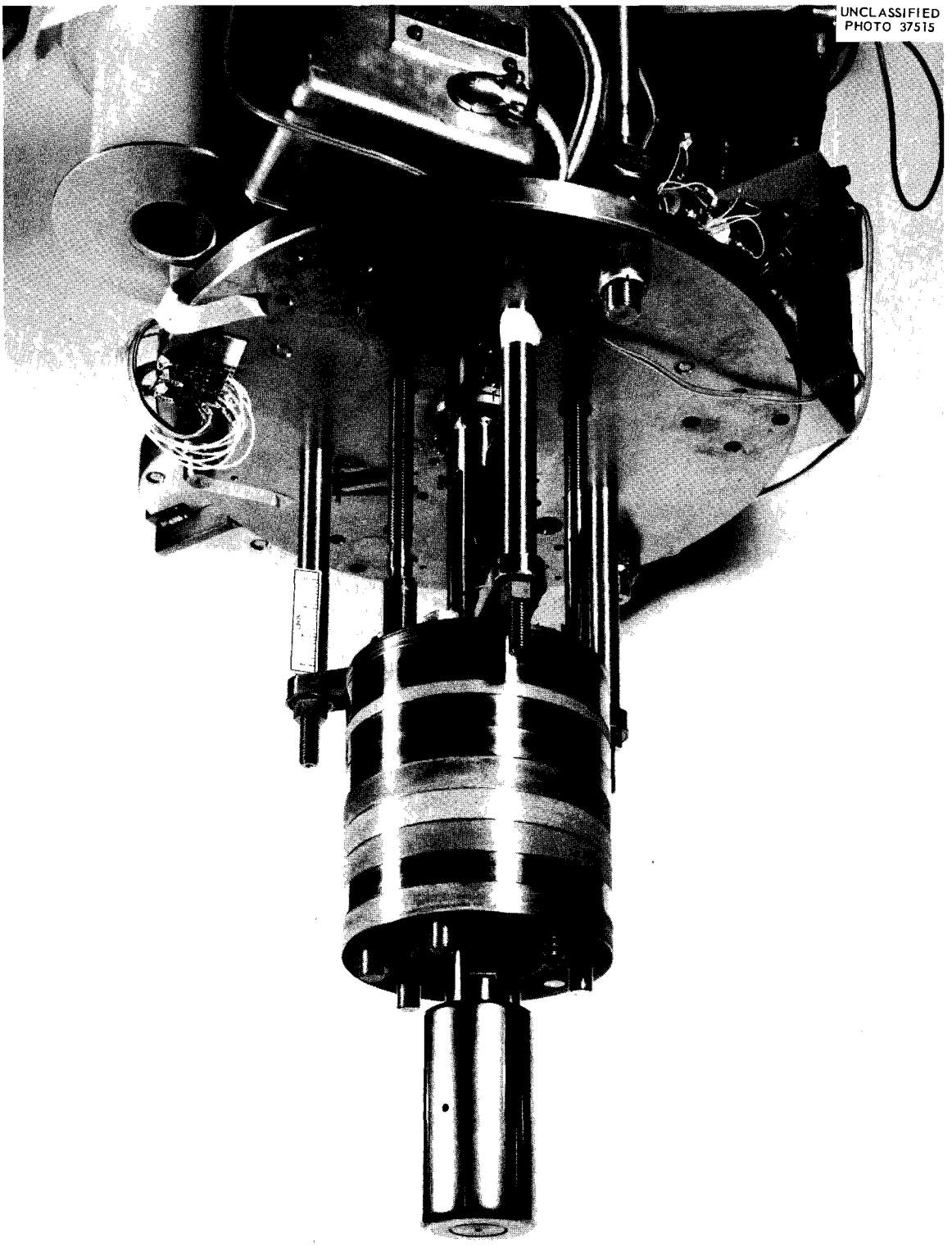

Fig. 2. ORNL Health Physics Research Reactor.

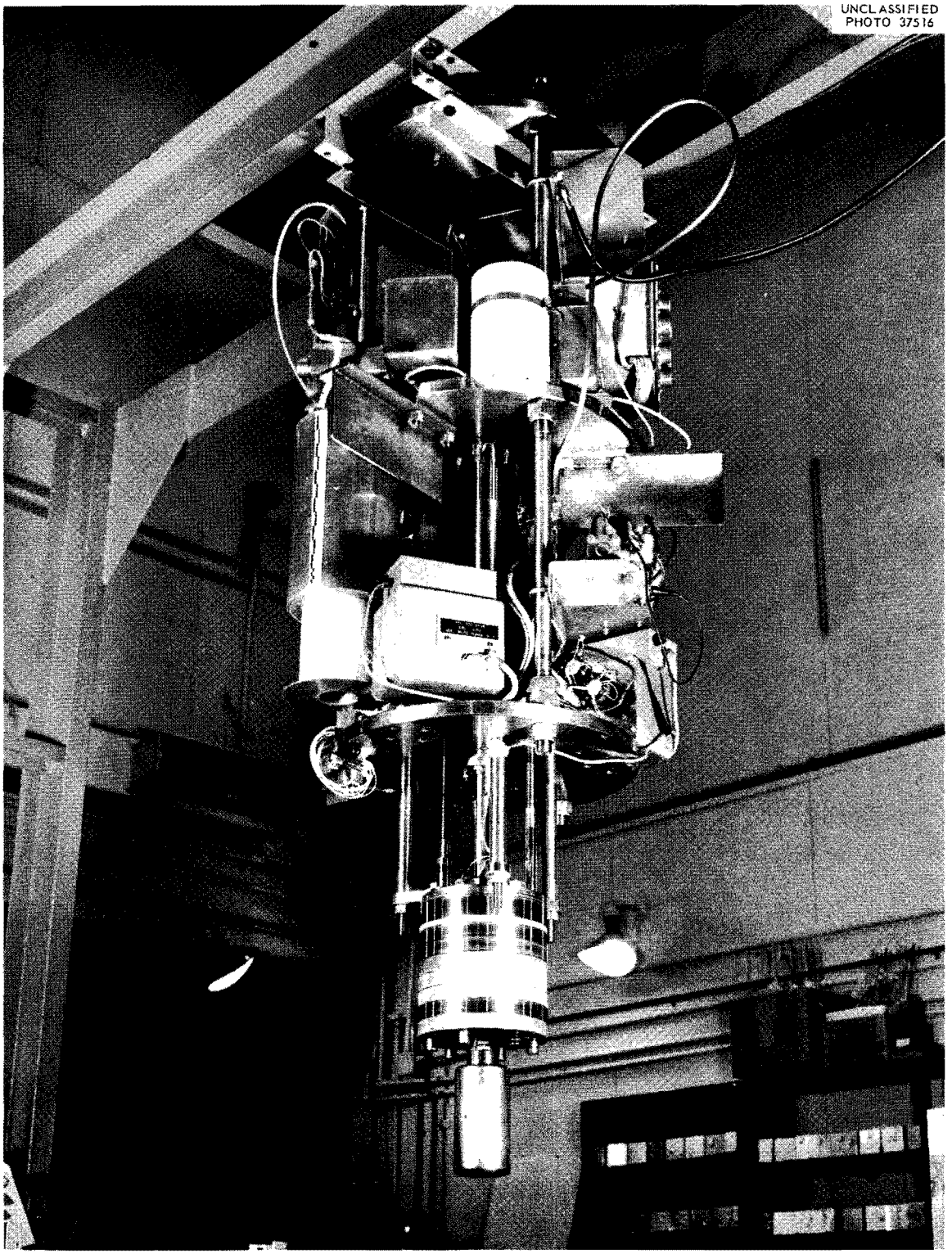

Fig. 3. ORNL Health Physics Research Reactor.

holding the steel core upward to insert the safety block in the reactor. As it moves upward, it compresses a spring which, when the magnet is de-energized, ejects the safety block with an acceleration of 2.28 g.

Two uranium-molybdenum control rods, worth 195 and 83 cents, respectively, are positioned by motors to achieve delayed critical. Neutron bursts are produced by rapid pneumatic insertion of a third rod. Although the full worth of this rod is $1.15, during the present work a part of the rod was fixed in the core and only the remainder of its length was used for burst production resulting in a reactivity change of about $1.00.

Burst Operation

The production of a typical burst began with a low-power run with the burst rod partially inserted, during which a rod configuration was established which gave the system a known amount of positive reactivity. The level of reactivity was determined by measurement of its associated stable period. The safety block was then retracted for about 20 minutes, allowing the neutron population to decay. With the external neutron source removed the safety block was then reinserted, increasing the reactivity to as much as 11 cents above delayed critical, and the burst rod immediately "fired" into the core, making the assembly super-prompt critical. The resulting power excursion was quenched by thermal expansion of the core and the residual plateau power level was terminated by removal of the safety block. The thermal shock resulting from bursts of $> \sim 6 \times 10^{16}$ fissions separated the steel core from its supporting magnet, automatically removing the safety block from the assembly; however, the acceleration of the safety block was not significantly greater than that in a normal instrument-actuated scram.

Instrumentation

The stable reactor period during the low-power run prior to burst production was obtained from measurements, made with three BF_3 proportional counters, of the count rate as a function of time.

Time behavior of the leakage flux was observed by means of a ~25-cm-OD, ~25-cm-long cylindrical plastic (polystyrene with terphenyl and POPOP) scintillation detector. The scintillator, viewed by a high-current photocell, was placed about 90 cm from the assembly to minimize the effect of scattered radiation and is shown in Fig. 4. The output current from the photocell was fed through terminated coaxial cable to produce vertical deflections in several camera-equipped oscilloscopes. Linear horizontal sweep rates and vertical amplifications were varied to best display the burst under observation. Triggering of the scope sweep was effected by a voltage pulse generated by a small scintillation counter when the incident flux exceeded a predetermined level. Camera shutters were triggered manually.

The total fission yield of each burst was obtained by measuring the P^{32} beta activity induced in each of three compressed sulfur pellets located respectively 0, 86, and 183 cm from the reactor surface. Sulfur activation was calibrated in terms of total fission yield by comparison with the results of radiochemical fission-product analyses of a uranium-molybdenum sample exposed in the vertical irradiation hole of the reactor. The ratio between the fission density in the sample and the total number of fissions in the reactor was obtained from the fission distribution calculated by Kinney which had agreed with the limited available experimental measurements.[2] The data from which the fission yields were determined are given in the appendix.

The fission rate in terms of the photocell output was determined by measuring the entire time-voltage integral of a burst trace up to the scram point and equating it to the number of fissions determined from sulfur activation. The photocell output was calibrated in this way for each run in which a burst trace up to scram time was obtained. When a trace was terminated earlier, the ratio of its peak signal to that of a fully calibrated run was used to determine the photocell output.

The reactor period for a burst was determined from the early part of the rise in the fission-rate trace before the temperature of the assembly increased.

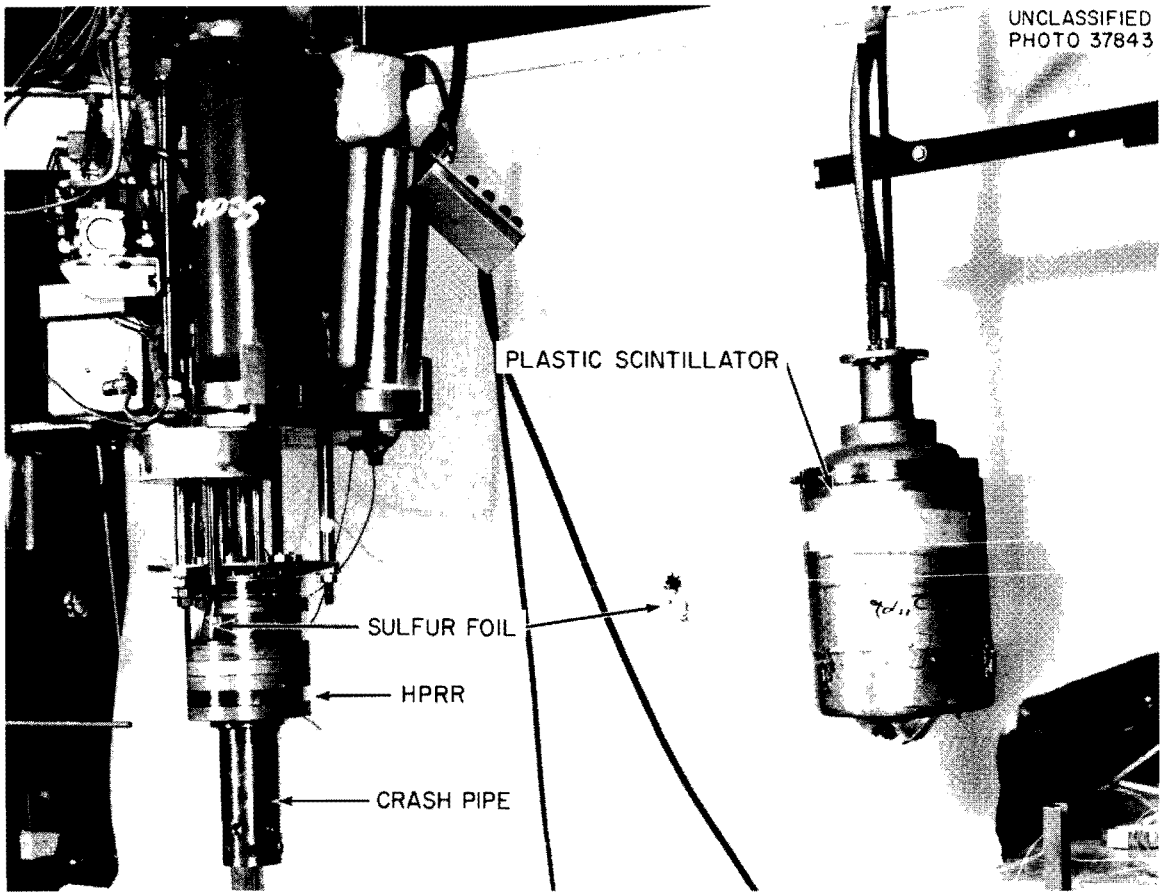

Fig. 4. ORNL Health Physics Research Reactor and Scintillation Detector.

Two iron-constantan thermocouples attached to two of the annular disks that make up the core measured the temperature. The thermocouple leads were brazed into brass plugs which were tightly screwed into the disks. The output was displayed on a recorder so that both the initial temperature and the curve of cooling following a burst could be observed. The eccentric locations of the thermocouples in the reactor, shown in Fig. 1, resulted in temperature measurements which were calculated to be 7% and 15% below the true peak temperature of the reactor. The temperature changes given below have been corrected, by computations based on calculated fission distributions and thermocouple positions, to true peak temperature changes. The calculated fission distribution indicates that the peak-to-average power density ratio is 1.9.

Results

The reciprocal positive reactor period, α, measured during the early part of a burst, is plotted in Fig. 5 as a function of the reactivity of the assembly after insertion of the burst rod. The intercept with the abscissa of a straight line, obtained by a linear least-squares fit of the data, shows that the prompt-critical condition was 0.25 cents above the reactivity of the burst rod. Thus, the reactivity associated with the burst rod stroke was 99.75 $\pm$ 0.25 cents. The slope of the line, according to the space-independent, one-velocity theory given by Wimett et al.,[3] is the prompt-neutron decay constant at delayed critical, α_p. The value of α_p obtained by a least-squares analysis of the data for all reciprocal periods larger than 10^{-4} sec^{-1} is $(0.55 \pm 0.03) \times 10^6$ sec^{-1}. This is to be compared with a value of 0.67×10^6 sec^{-1} calculated by W. E. Kinney assuming 0.007 as the effective fraction of delayed neutrons. The computation is based on a value of the prompt-neutron lifetime of 1.04×10^{-8} sec, which was calculated by perturbation theory using the angular fluxes from an S_4 transport theory code.[2] The effect of neutrons returned to the assembly by the walls and floor of the room may be the reason for the difference between the experimental and calculated values of α_p in the present work.

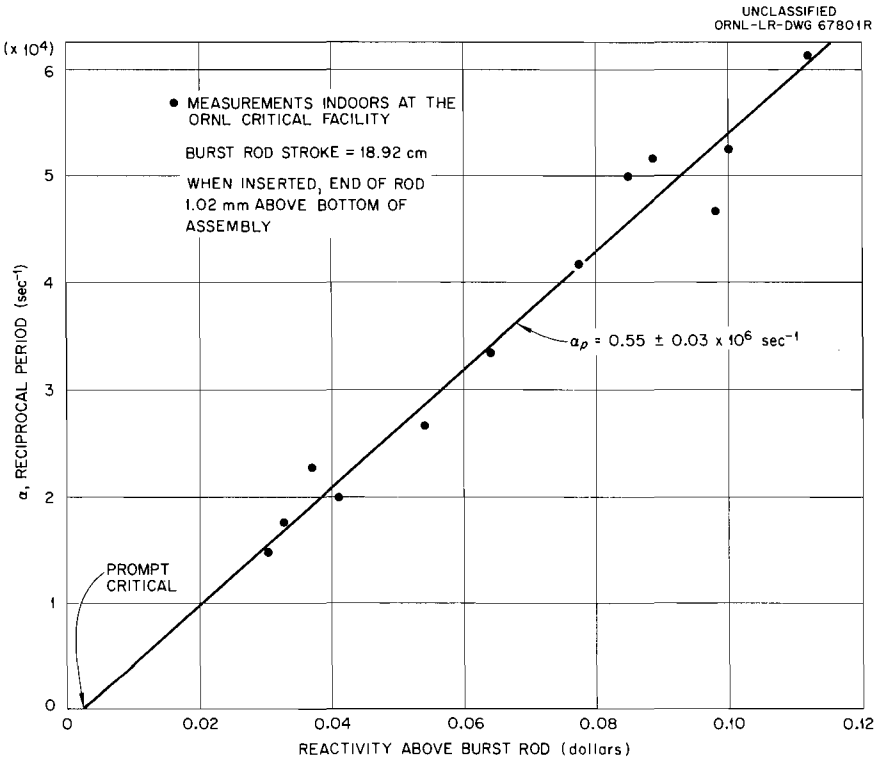

Fig. 5. Reciprocal Reactor Period as a Function of Reactivity Above Burst Rod for the HPRR.

Some typical burst traces, replotted from the oscilloscope photographs, are shown in Figs. 6, 8, 9, and 10. Other burst traces obtained are included in Appendix B. Zero time is always arbitrary. The figures also list reactor period, burst half width, peak fission rate, and the total fission yield.

In the burst of Fig. 6, the residual plateau is quite evident. From the burst shape, the temperature rise, the calculated peak-to-average power density distribution, and the reactivity above prompt critical required to produce the burst, the average dynamic temperature coefficient for the burst of Fig. 6 was computed to be 0.31 cents/°C. Also shown on this figure are the time of initial safety block motion, obtained from the signal of a transducer attached to the block, and the reactivity associated with its displacement as a function of time. The latter quantity was readily obtained from the known reactivity of the block as a function of displacement (80 cents/cm over the first 2.5 cm) and the known motion of the block as a function of time after release.

In the actual oscilloscope photograph of Fig. 7, a burst of somewhat greater yield than that of Fig. 6 is shown. Oscillations of the amplitude of the residual plateau are visible. These oscillations stem from the vibration in the plates of the assembly. This vibration is in the vertical direction with a frequency, according to the photograph, of about 5 kc/sec. It is apparently possible for this vibration to separate the core disks, since the bolts which hold the core together were loose during many experiments. Independent measurements of the vibration of the system following a burst indicate a frequency in the vertical direction of about 6 kc/sec, while the vibrational frequency in the radial direction was about 22 kc/sec.

Figure 8 shows a burst of 7.2×10^{16} fissions, where the pressure waves in the safety block have separated it from its magnet about 225 μsec after the peak of the burst. In four different bursts in which this shock-separation was observed, the time was found to be between 220 and 235 μsec after each peak.

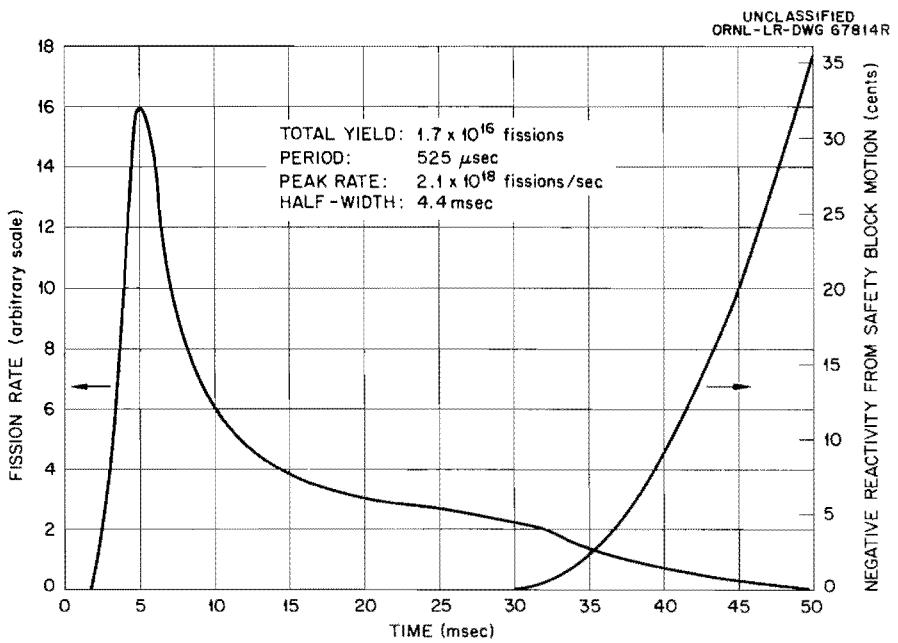

Fig. 6 Trace of Oscilloscope Photograph for a Burst of 1.7×10^{16} Fissions (HPRR).

UNCLASSIFIED
ORNL-LR-DWG 67802

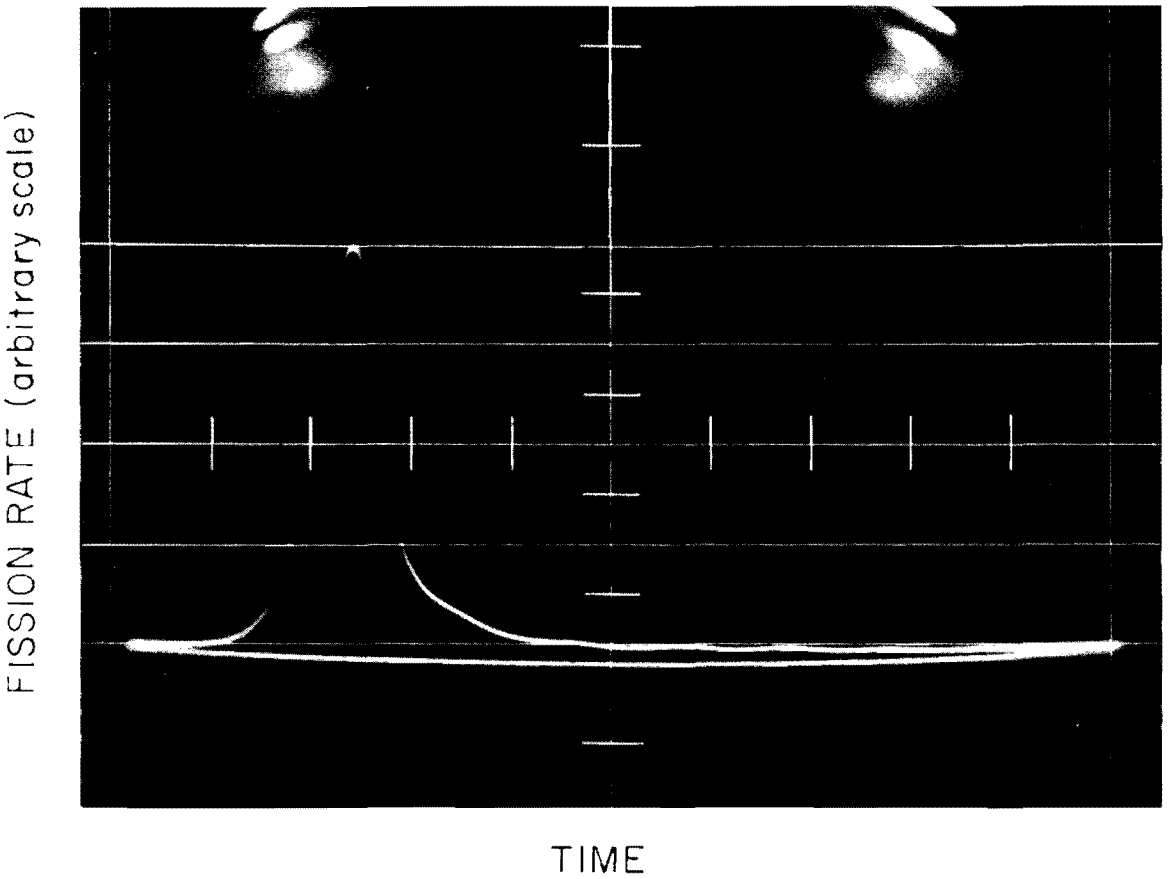

TIME SCALE: 217.4 μsec/division

TOTAL YIELD: 4×10^{16} fissions

PERIOD: 45 μsec

HALF-WIDTH: 175 μsec

PEAK RATE: 1.2×10^{20} fissions/sec

Fig. 7. Oscilloscope Photograph for a Burst of 4×10^{16} Fissions (HPRR).

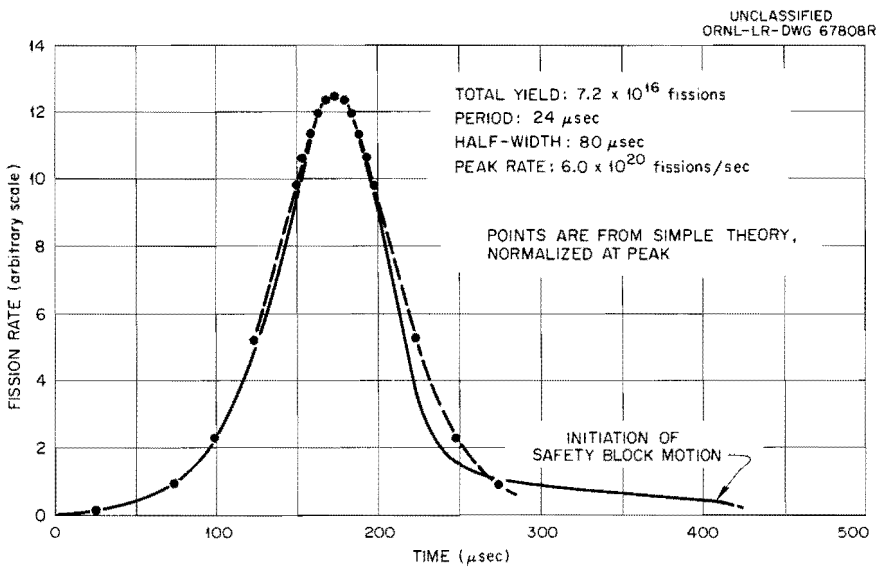

Fig. 8. Trace of Oscilloscope Photograph for a Burst of 7.2×10^{16} Fissions (HPRR).

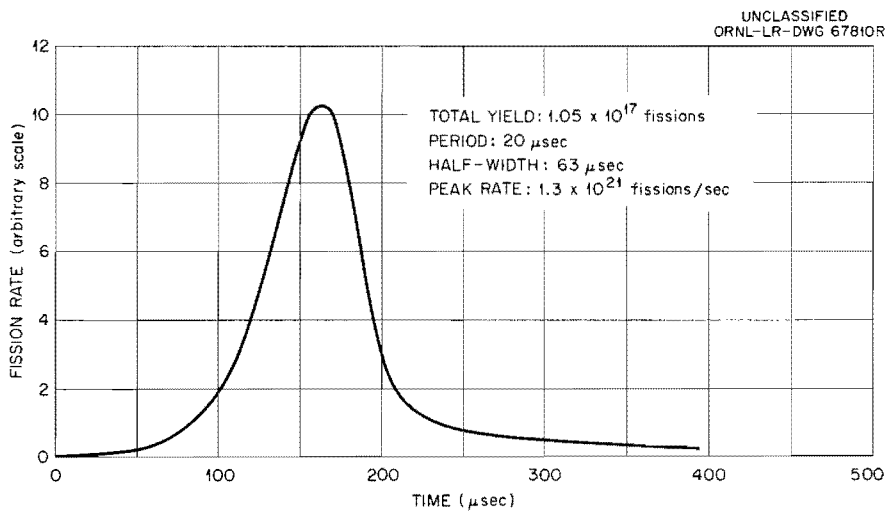

Fig. 9. Trace of Oscilloscope Photograph for a Burst of 1.05×10^{17} Fissions (HPRR).

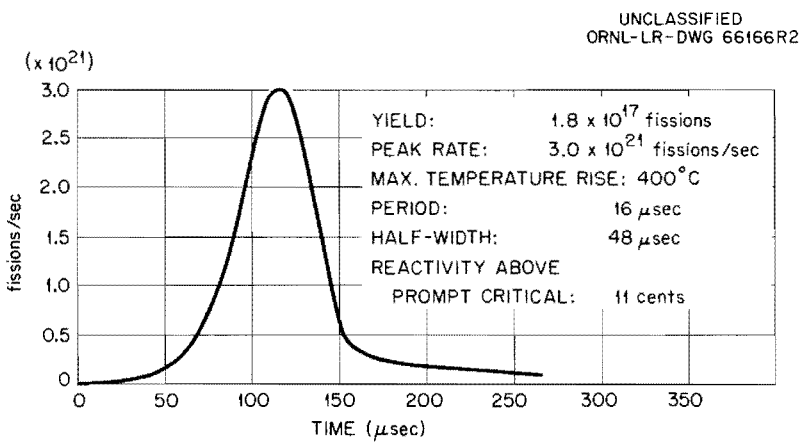

Fig. 10. Trace of Oscilloscope Photograph for a Burst of 1.8 x 10^{17} Fissions (HPRR).

~~Also shown in this figure is a theoretical burst shape, based on the one-group model previously noted. The curves have been normalized at their peaks. In all comparisons between theory and experiment, agreement appeared good in the rising part of the burst, but the neutron decay in the experiments was always faster than predicted by calculation. The calculation, however, assumes a constant temperature coefficient of reactivity. Since the coefficient of linear thermal expansion of the uranium-molybdenum alloy increases about 1% for every 20°C of temperature increase, the temperature coefficient of reactivity may actually be a function of system temperature, thus causing the burst to decay faster than predicted.~~

Figures 9 and 10 show bursts of 1.05×10^{17} and 1.8×10^{17} fissions, respectively.

In the burst of 1.8×10^{17} fissions, the peak temperature rise was 400°C. Although up to the time of the peak of the burst 45% of the fissions had occurred, the thermal expansion at that time was only sufficient to reduce the reactivity 11 cents. This indicates, as was expected, that the thermal expansion lags behind the energy release.

Fission yield versus temperature rise is plotted in Fig. 11. The calculated curve, obtained by using a specific heat of 0.042 cal/g.°C and a mass of 114.8 kg for the uranium-molybdenum alloy, and assuming 178 Mev/fission for the energy deposited in the core, gives 3.8×10^{14} fissions per centigrade degree temperature increase. The measured value is 4.6×10^{4} fissions/°C. A burst of 5.2×10^{17} fissions would raise the peak temperature in the assembly to 1150°C, the melting point of the alloy.

The peak fission rate as a function of reactor reciprocal period is shown in Fig. 12. Simple theory predicts that the peak fission rate is proportional to the square of the reciprocal period. The data deviate at both ends of the curve. For periods longer than 30 μsec the deviations are probably due to the effect of neutrons scattered back from the room walls and floor. For periods shorter than 30 μsec, more intense bursts than were predicted were obtained, because of the lag between fission energy release and expansion of the reactor volume.

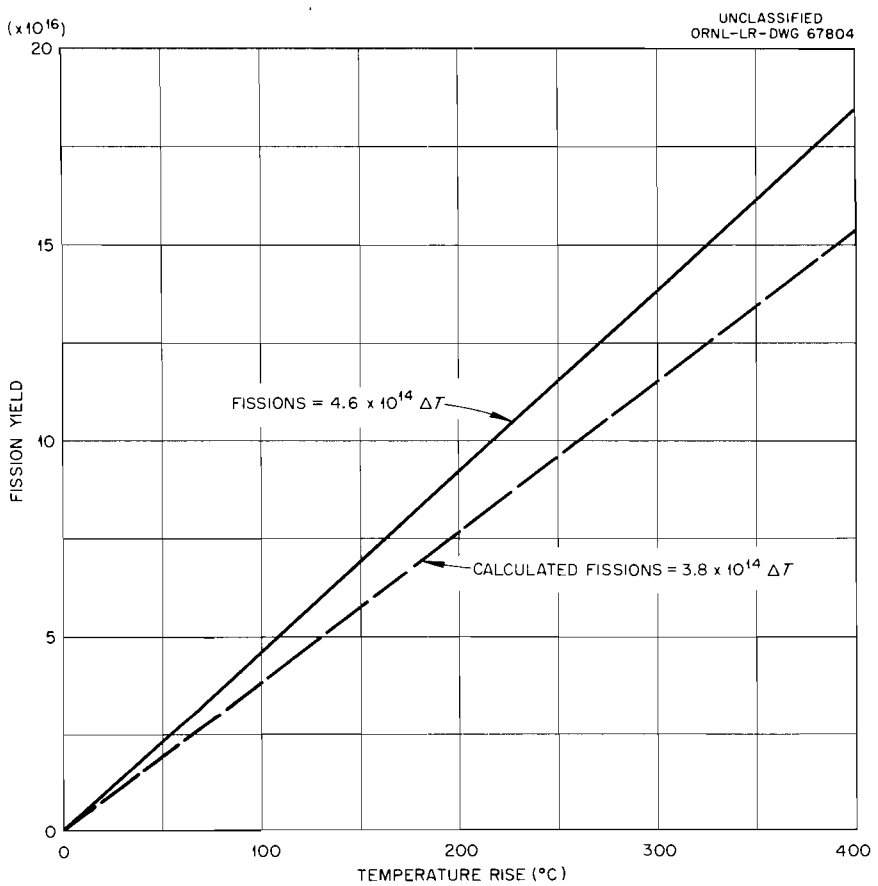

Fig. 11. Total Fission Yield as a Function of Temperature Rise in the HPRR.

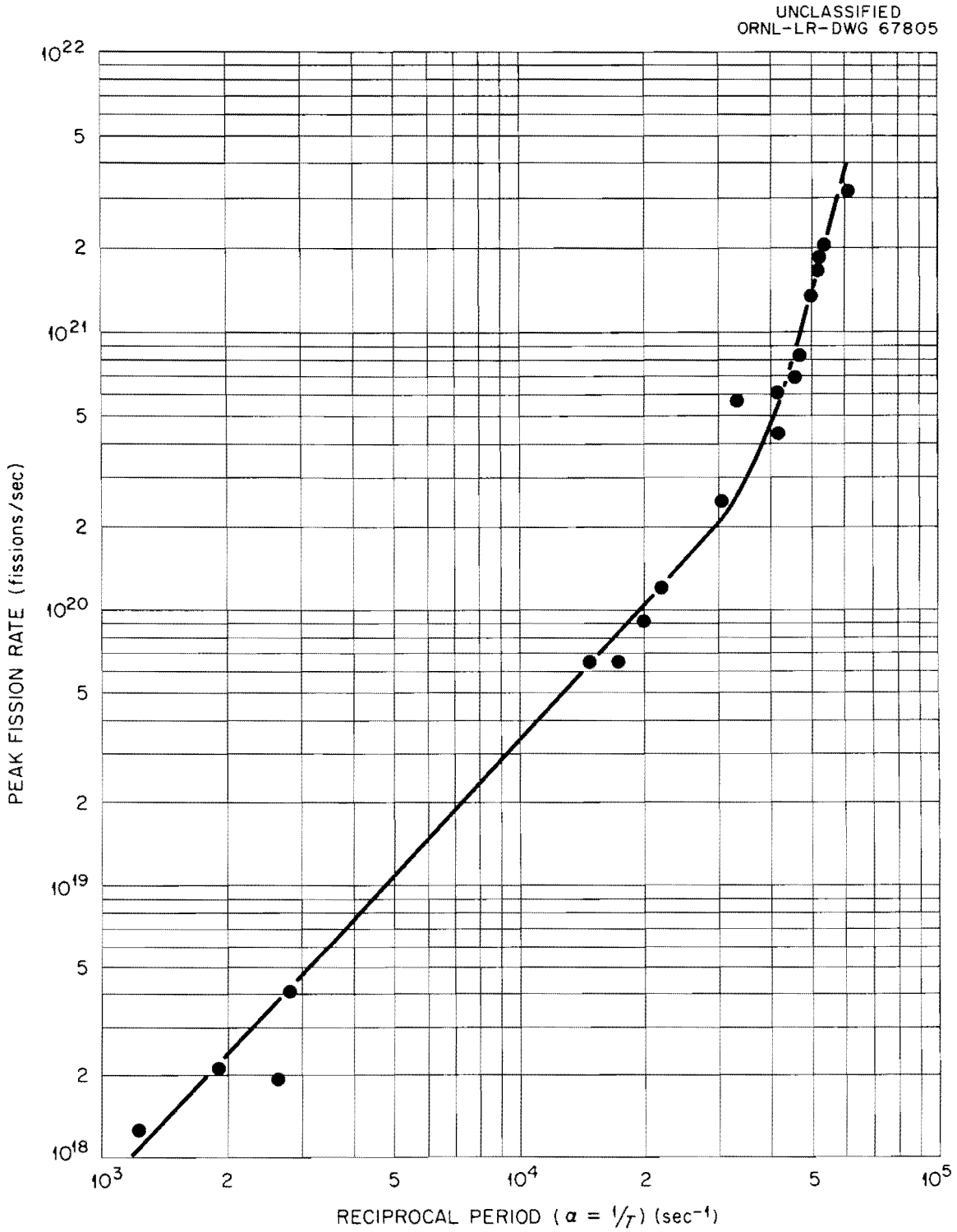

Fig. 12. Peak Fission Rate as a Function of Reactor Reciprocal Period (HPRR).

The total fission yield and the yield in the "spike" of the burst are shown as functions of reciprocal period in Fig. 13. The fission yield in the spike of the burst was obtained by graphical integration of the oscilloscope traces. In the higher yield bursts, about 90% of the fissions occur in the spike and 10% in the tail before the pressure waves generated in the burst scram the system.

Acknowledgements

The burst detection equipment was made available by the N-2 Group at Los Alamos Scientific Laboratory. The assistance of T. F. Wimett of LASL in the early phases of the experiment and in discussions of the results is acknowledged. Sulfur activations and counting were done by E. B. Johnson, and fission product analyses by the Radiochemical Analysis group under E. Wyatt. Co-workers in performing the experiments were L. W. Gilley, A. D. Callihan, J. J. Lynn, E. R. Rohrer, and J. F. Ellis. The work of J. R. Hill*in reactor control maintenance is also acknowledged.

*Instrumentation and Controls Division.

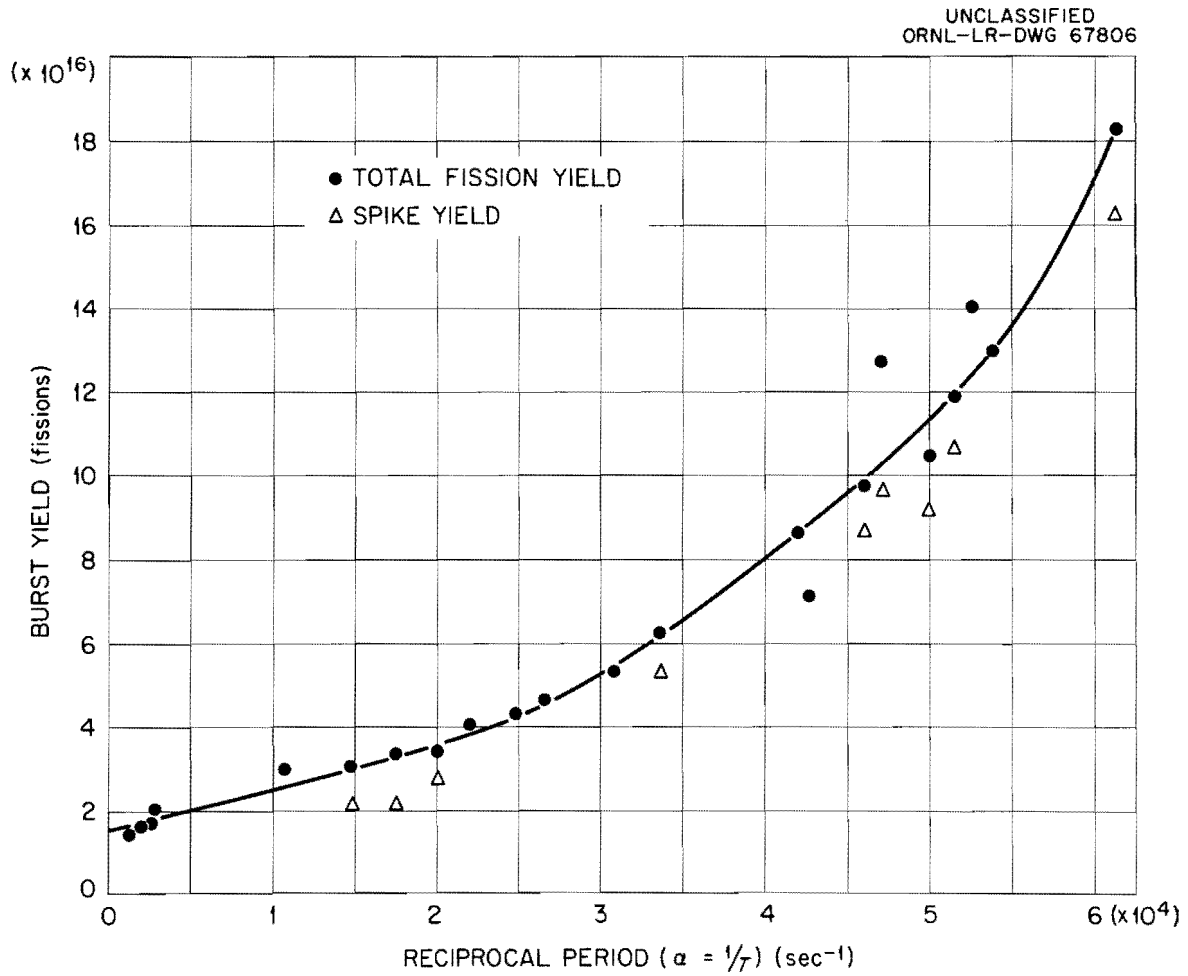

Fig. 13. Total Fission and "Spike" Yields as a Function of Reactor Reciprocal Period (HPRR).

Appendix A: Fission Yield Determination Data

The text has described the determination of fission yield from measurements of the beta activity of irradiated sulfur pellets. These pellets were 3.8 cm in diameter and 0.95 cm thick. Their orientations with respect to the core are as shown in Fig. 4. The scintillation counter used to measure the pellet activity had been calibrated in the manner described by Reinhardt and Davis[4] and by Hurst and Ritchie.[5] Where possible during the present experiments individual pellets were counted both before and after burning, and the quoted flux is the average of the two counts.

Table A-1 shows the results of five fission-product analyses used to calibrate the sulfur activity in terms of the total fission yield. In these runs fission yield was determined by exposing rods of alloy in the irradiation hole of the reactor and radiochemically analyzing the samples, after exposure, for fission-product activity. Barium-140 production was used as the index in the fission-product determinations. The number of fissions per unit flux was at points 0, 86, and 183 cm from the reactor. It may be noted that at each position the maximum spread of values is less than 20%. The average of these values shown in the table were applied to the sulfur flux data of subsequent runs to determine the fission yields given in Table A-2.

---

4. P. W. Reinhardt and F. J. Davis, Health Physics, 1, 169-175 (1958).
5. G. S. Hurst and R. H. Ritchie, Radiation Accidents: Dosimetric Aspects of Neutron and Gamma-Ray Exposure, ORNL-2748, Part A (May, 1961).

*A Ba^{140} fission yield of 6.1% was used.

Table A-1. Calibration of Sulfur Pellets in Terms of Fission Yield

Run Number	Yield (fissions)*	Integrated Flux ($n \cdot cm^{-2}$) Position No. 1	Position No. 2	Position No. 3	Fissions per unit Flux Position No. 1	Position No. 2	Position No. 3
	$\times 10^{16}$	$\times 10^{12}$	$\times 10^{10}$	$\times 10^{9}$	$\times 10^{3}$	$\times 10^{5}$	$\times 10^{6}$
0	1.96	3.94	5.48	8.25	4.96	3.57	2.37
15	6.63	12.6	18.3	32.3	5.26	3.62	2.05
36	5.60	9.36	13.4	24.2	5.99	4.18	2.31
37	8.00	15.3	21.8	39.3	5.22	3.67	2.03
38	9.48	17.2	24.5	44.2	5.51	3.87	2.14
Average					5.38	3.78	2.41

*Determined by radiochemical fission-product analyses.

Table A-2. Fission Yields from Various Bursts, Determined from Sulfur Pellet Activations

Integrated Flux ($n.cm^{-2}$)			Total Yield (fissions)
Position 1	Position 2	Position 3	
$\times 10^{12}$	$\times 10^{10}$	$\times 10^{9}$	$\times 10^{16}$
0.17	0.24	0.42	0.096
0.70	1.09	1.92	0.42
2.27	3.38	6.58	1.32
2.52	3.71	-	1.46
2.95	4.32	7.51	1.68
2.93	4.32	7.68	1.69
3.37	4.89	7.50	1.84
3.58	5.20	9.47	2.06
3.99	5.37	9.73	2.18
4.31	5.94	9.90	2.33
5.34	7.78	13.0	2.99
5.45	7.67	14.1	3.08
5.91	8.39	15.2	3.34
6.01	8.60	15.6	3.42
7.15	10.1	18.0	4.01
7.46	10.9	-	4.30
7.91	11.8	-	4.61
9.36	13.4	24.2	5.32
11.5	15.3	28.2	6.26
12.6	18.3	32.2	7.17
15.3	21.8	39.3	8.66
15.9	22.9	42.4	9.15
17.2	24.5	44.2	9.73
19.2	25.8	47.3	10.5
21.2	30.6	52.2	11.9
23.8	30.6	57.6	12.7
22.4	34.0	58.2	13.0
	34.1	62.9	14.0
	43.7	83.5	18.3

Appendix B: Oscilloscope Burst Traces

Traces of oscilloscope photographs for bursts ranging from 3.1×10^{16} fissions to 1.3×10^{17} fissions are presented on the following pages.

Total Yield	Page No.
3.1×10^{16} fissions	26
3.4×10^{16} fissions	27
6.3×10^{16} fissions	28
8.7×10^{16} fissions	29
9.7×10^{16} fissions	30
1.2×10^{17} fissions	31
1.3×10^{17} fissions	32

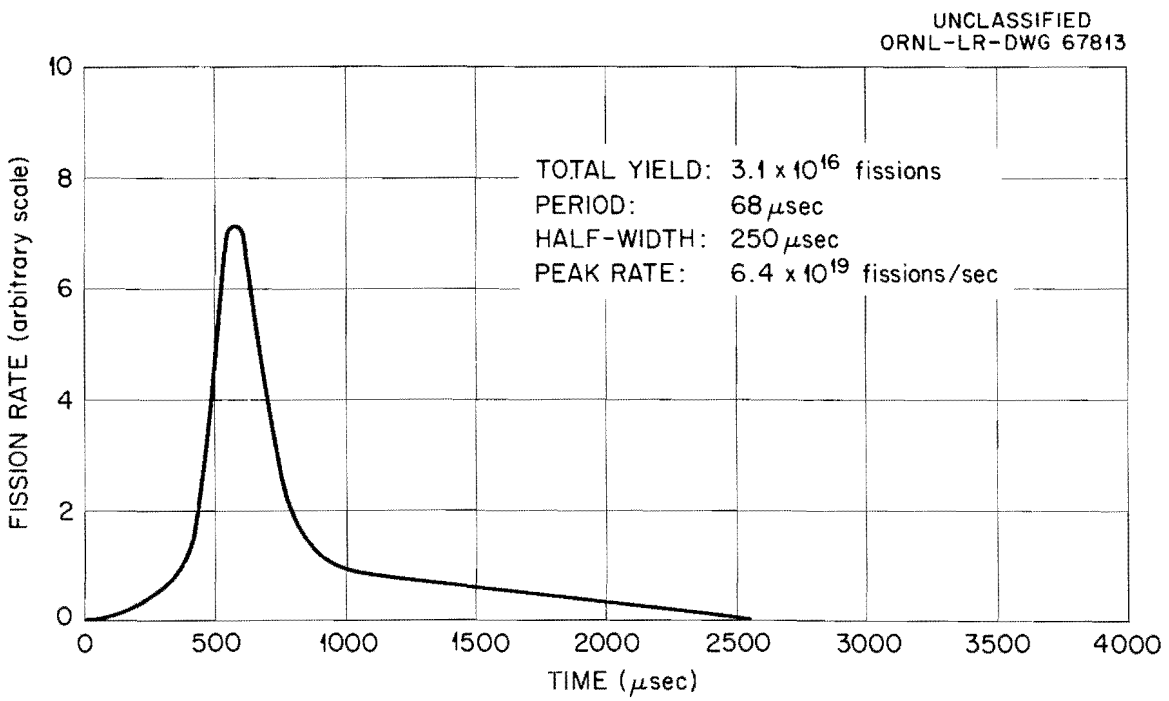
UNCLASSIFIED
ORNL-LR-DWG 67813
TOTAL YIELD: 3.1 x 10^16 fissions
PERIOD: 68 μsec
HALF-WIDTH: 250 μsec
PEAK RATE: 6.4 x 10^19 fissions/sec
FISSION RATE (arbitrary scale)
TIME (μsec)
0
2
4
6
8
10
0
500
1000
1500
2000
2500
3000
3500
4000

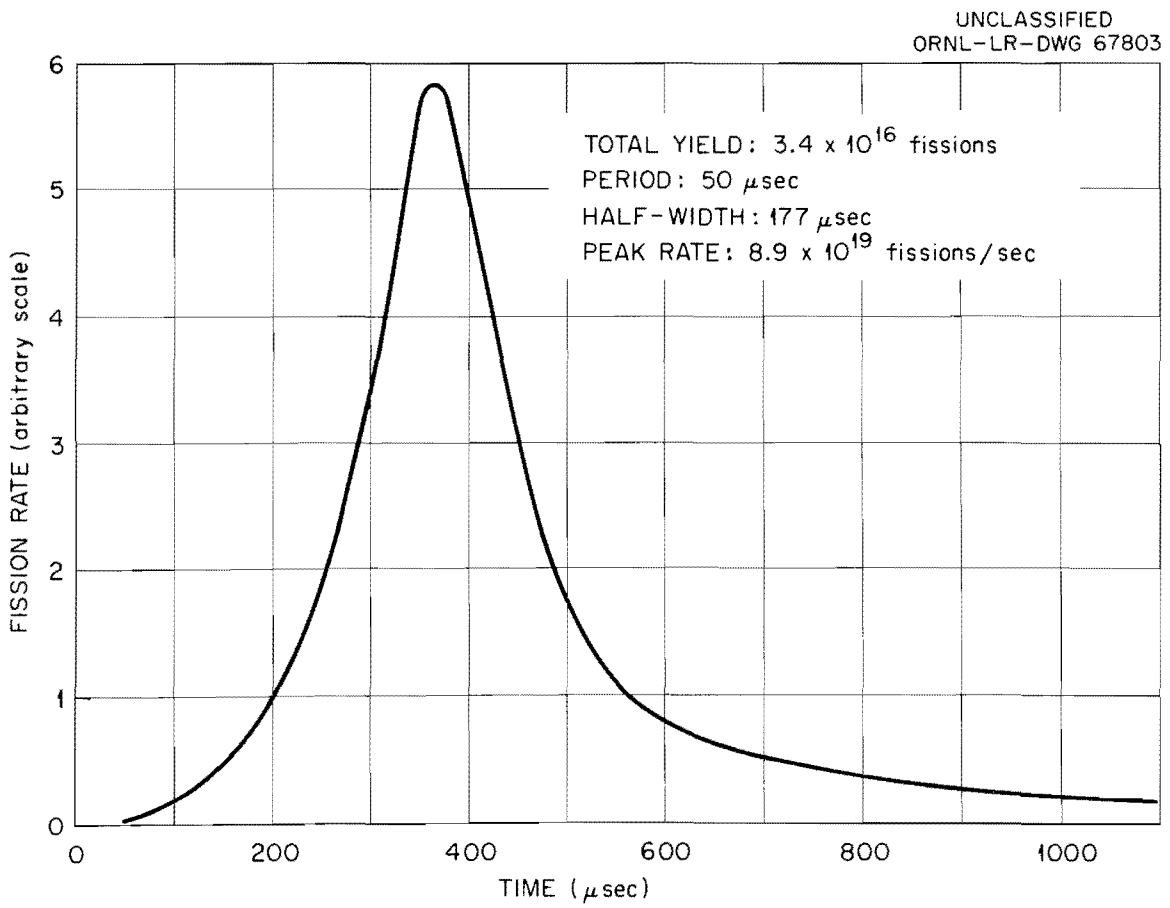
UNCLASSIFIED
ORNL-LR-DWG 67803
TOTAL YIELD: 3.4 x 10^16 fissions
PERIOD: 50 μsec
HALF-WIDTH: 177 μsec
PEAK RATE: 8.9 x 10^19 fissions/sec
FISSION RATE (arbitrary scale)
0
1
2
3
4
5
6
0
200
400
600
800
1000
TIME (μsec)

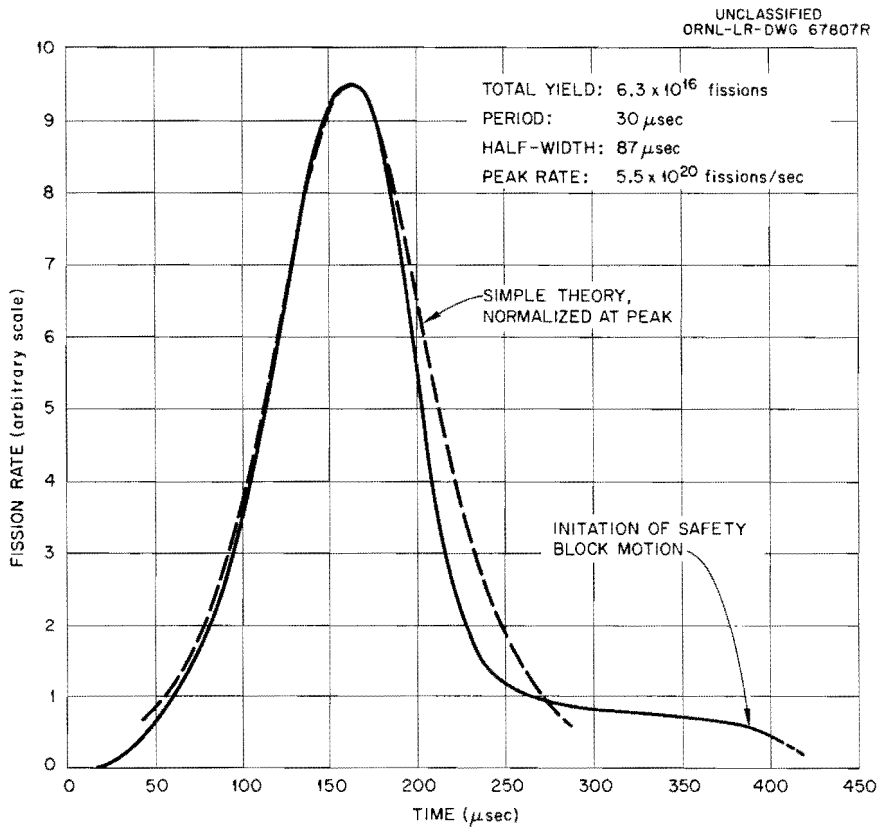
UNCLASSIFIED
ORNL-LR-DWG 67807R
TOTAL YIELD: 6.3 x 10^16 fissions
PERIOD: 30 μsec
HALF-WIDTH: 87 μsec
PEAK RATE: 5.5 x 10^20 fissions/sec
SIMPLE THEORY, NORMALIZED AT PEAK
INITATION OF SAFETY BLOCK MOTION
FISSION RATE (arbitrary scale)
TIME (μsec)
0
1
2
3
4
5
6
7
8
9
10
0
50
100
150
200
250
300
350
400
450

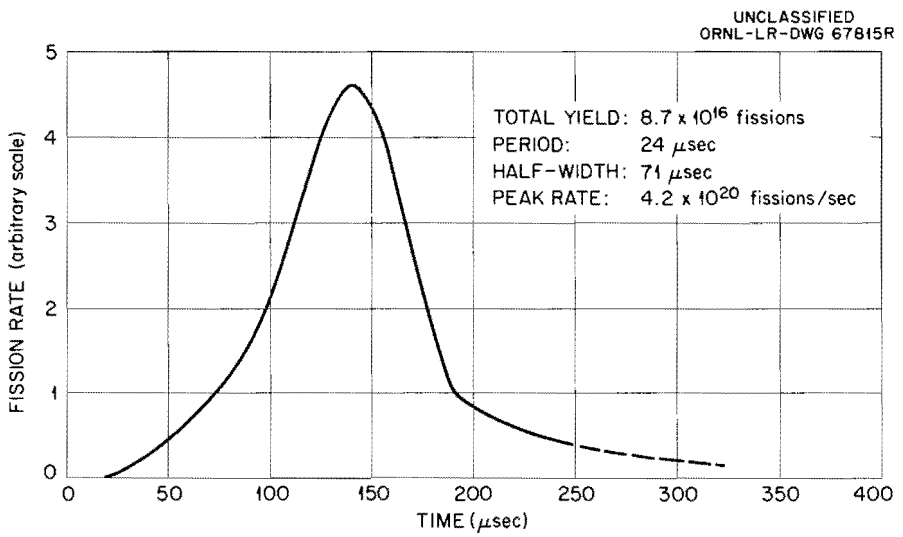
UNCLASSIFIED
ORNL-LR-DWG 67815R
TOTAL YIELD: 8.7 x 10^16 fissions
PERIOD: 24 μsec
HALF-WIDTH: 71 μsec
PEAK RATE: 4.2 x 10^20 fissions/sec
FISSION RATE (arbitrary scale)
TIME (μsec)
0
1
2
3
4
5
0
50
100
150
200
250
300
350
400

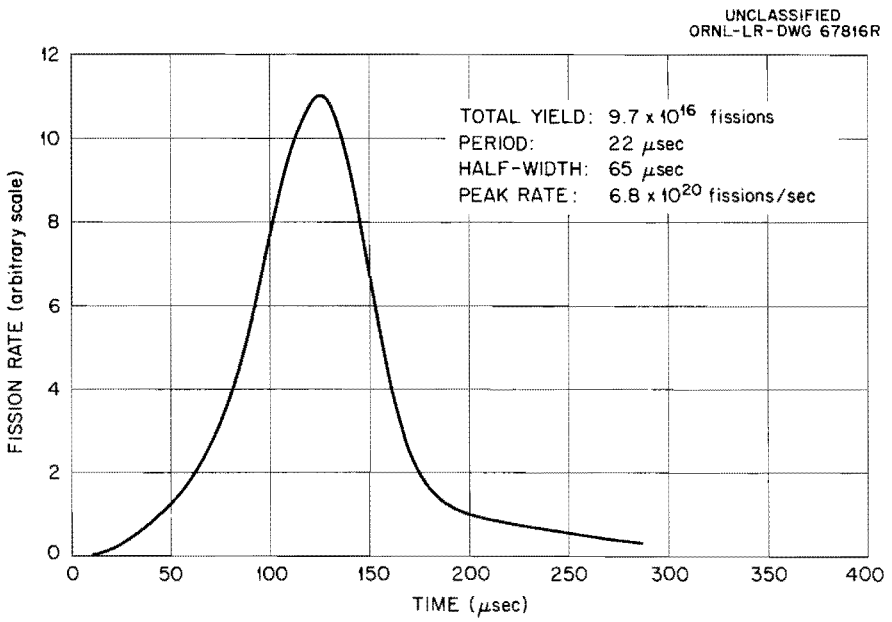
UNCLASSIFIED
ORNL-LR-DWG 67816R
TOTAL YIELD: 9.7 x 10^16 fissions
PERIOD: 22 μsec
HALF-WIDTH: 65 μsec
PEAK RATE: 6.8 x 10^20 fissions/sec
FISSION RATE (arbitrary scale)
TIME (μsec)
0
2
4
6
8
10
12
0
50
100
150
200
250
300
350
400

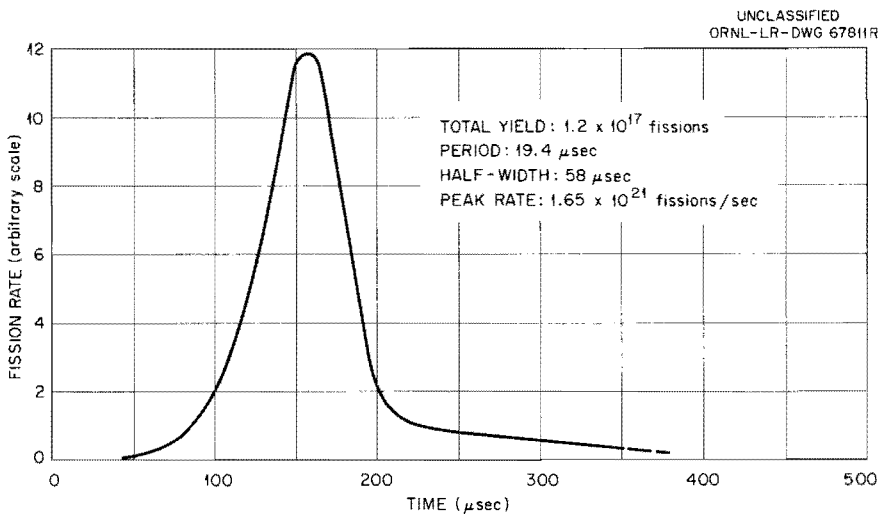
UNCLASSIFIED
ORNL-LR-DWG 67811R
TOTAL YIELD: 1.2 x 10^17 fissions
PERIOD: 19.4 μsec
HALF-WIDTH: 58 μsec
PEAK RATE: 1.65 x 10^21 fissions/sec
FISSION RATE (arbitrary scale)
TIME (μsec)
0
2
4
6
8
10
12
0
100
200
300
400
500

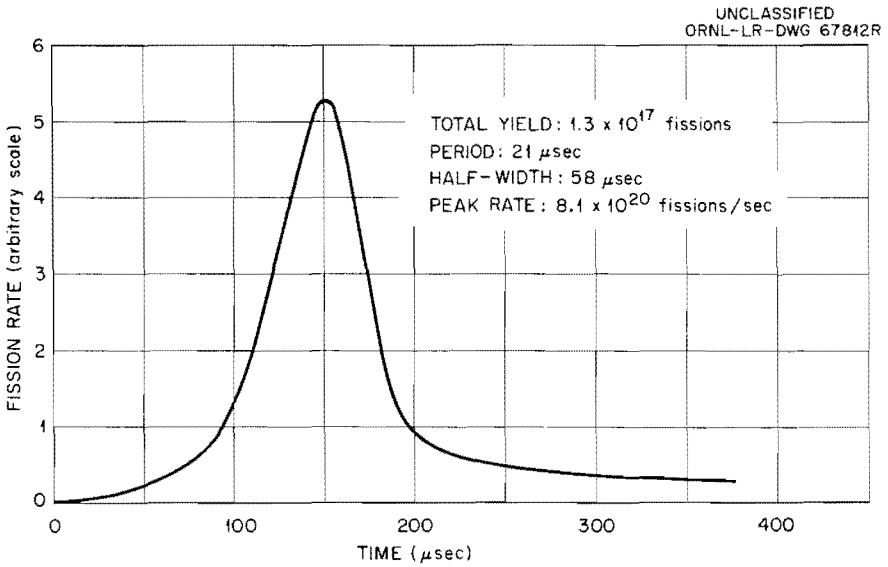
UNCLASSIFIED
ORNL-LR-DWG 67842R
TOTAL YIELD: 1.3 x 10^17 fissions
PERIOD: 21 μsec
HALF-WIDTH: 58 μsec
PEAK RATE: 8.1 x 10^20 fissions/sec
FISSION RATE (arbitrary scale)
TIME (μsec)
0
1
2
3
4
5
6
0
100
200
300
400

Internal Distribution

1. J. L. Anderson
2. J. A. Auxier
3. E. P. Blizard
4. R. C. Block
5. T. V. Blosser
6. A. L. Boch
7. F. R. Bruce
8. T. J. Burnett
9-18. A. D. Callihan
19. T. E. Cole
20. R. R. Coveyou
21. G. deSaussure
22. E. P. Epler
23. J. K. Fox
24-28. L. W. Gilley
29. E. E. Gross
30. R. Gwin
31. D. C. Hamilton
32. S. H. Hanauer
33. J. A. Harvey
34. K. M. Henry
35. J. R. Hill
36-37. L. B. Holland
38. C. F. Holloway
39. G. S. Hurst
40. E. B. Johnson
41. W. H. Jordan
42. P. R. Kasten
43. W. E. Kinney
44. J. A. Lane
45. M. I. Lundin
46. J. J. Lynn
47. J. D. McLendon (Y-12)
48. H. G. MacPherson
49. D. W. Magnuson
50. F. C. Maienschein
51-65. J. T. Mihalczo
66. K. Z. Morgan
67. F. J. Muckenthaler
68. C. W. Nestor
69. L. C. Oakes
70. R. W. Peelle
71. A. M. Perry
72. P. H. Pitkanen
73. D. P. Roux
74. E. G. Silver
75. M. J. Skinner
76. M. L. Tobias
77. D. R. Ward
78. A. M. Weinberg
79. F. G. Welfare (Y-12)
80. W. Zobel
81-83. Laboratory Records
84. Laboratory Records, ORNL R.C.
85-86. Central Research Library
87. Document Reference Section
88. Research and Development Division, ORO
89-103. Division of Technical Information Extension, DTIE

External Distribution

104-106. United Nuclear Corporation, White Plains, New York
107. J. R. Beyster; General Atomic, San Diego, California
108-112. H. C. Paxton, G. E. Hansen, C. B. Mills, W. R. Stratton, and T. F. Wimett; Los Alamos Scientific Laboratory, Los Alamos, New Mexico
113-116. J. E. Carothers, E. H. Cristie, G. E. Cummings, and O. C. Kolar; University of California, Lawrence Radiation Laboratory, Livermore, California
117-118. D. M. Ellett and P. D. O'Brien; Sandia Corporation, Albuquerque, New Mexico
119. C. L. Schuske; Dow Chemical Company, Rocky Flats, Colorado
120. E. O. Baicy, U.S. Army Ordnance Ballistics Laboratory, Aberdeen Proving Grounds, Aberdeen, Maryland
121. G. E. Elder; White Sands Missile Range, White Sands, New Mexico
122. A. L. Kaplan; General Electric Corp, Syracuse, New York
123. E. D. Clayton; General Electric Company, Hanford Laboratories, Richland, Washington
124. D. Wood; Albuquerque Operations Office, Atomic Energy Commission, Albuquerque, New Mexico